

Photocatalytic activity of Hibiscus leaf extract mediated ZnO nanoparticles by hydrothermal method

S. Roselin Mariyal¹, G. Nedunchezian³, D. Benny Anburaj¹, S. Joshua Gnanamuthu²

¹P. G. and Research Department of Physics, D.G. Govt Arts College (Affiliated to Bharathidasan University), Mayiladuthurai, India

²P. G. and Research Department of Physics, TBML College (Affiliated to Bharathidasan University), Porayar, India

³P. G. and Research Department of Physics Thiru. Vi. Ka. Govt Arts College (Affiliated to Bharathidasan University), Thiruvarur, India

Corresponding author: S. Joshua Gnanamuthu, joshuagnanamuthu@gmail.com

ABSTRACT *Hibiscus* leaf extract mediated ZnO nanoparticles have been prepared through a hydrothermal method and the effects of extract doping on the structural, optical and electronic properties of ZnO NPs were studied. The photocatalytic oxidation of methylene blue dye under visible light irradiation was used to determine the photocatalytic performance of the prepared nanoparticles. The extracted ZnO nanoparticles (R₃) exhibited the lowest band gap and the highest photocatalytic activity for the methylene blue dye. The photocatalytic performance of the (R₃) prepared ZnO nanoparticles was stable after the nanoparticles were reused five times for the oxidation of methylene blue dye.

KEYWORDS Photocatalysis, hydrothermal method

FOR CITATION Mariyal S.R., Nedunchezian G., Anburaj D.B., Gnanamuthu S.J. Photocatalytic activity of Hibiscus leaf extract mediated ZnO nanoparticles by hydrothermal method. *Nanosystems: Phys. Chem. Math.*, 2022, **13** (4), 430–437.

1. Introduction

Synthetic dyes used in the textile and dye industries account for a large proportion of pollutants in wastewater. Most of the organic dyes used are difficult to degrade, resulting in irreversible damage to the environment [1]. Although many efficient approaches have been applied to manage this problem, including membrane separation, adsorption, coagulation and microbial degradation [2], these methods have many disadvantages, such as generation of secondary pollution, refractory degradation products and high costs, all of which lead to great limitation in practical application [3–5]. Recently, photocatalytic degradation of organic dyes using semiconductors has attracted great attention [6]. This refers to the process in which organic compounds are gradually oxidized into inorganic compounds or even H₂O and CO₂ under the synergistic effects of light and photocatalysis.

ZnO is one of the most suitable catalysts in many industries given its inexpensive, non-toxic, efficient and anti-corrosion properties [7]. Nevertheless, it still has some disadvantages with respect to photocatalysis. For example, it has a narrow response range, low quantum efficiency, and its photogenerated electron-hole pairs are easy to recombine. The photocatalytic performance can be greatly affected by the particle size, morphology and concentration [8, 9]. As such, it is possible to modify these ZnO properties to enhance its photocatalytic efficiency. Doping ZnO with rare-earth ions is an attractive strategy to improve its photocatalytic activity by modifying its surface morphology [10, 11].

ZnO NPs can be synthesized by various chemical and physical routes including the hydrothermal method, the sol-gel method, the laser ablation method, the sonochemical technique, the mechanochemical method and the microwave technique [10–14]. However, some of these methods require high pressure and high temperature, while others require inert atmosphere and toxic chemicals [15]. In addition, these routes include complex and expensive synthesis and purification processes making them less preferable.

Recently, a biological synthesis of ZnO NPs via micro-organisms and plant extracts has been developed as an alternative to chemical and physical routes due to its cost effectiveness, simple handling, nontoxicity and eco-friendly nature [16, 17]. Therefore, in this work, we study the effects of different concentrations of the extract of the *Hibiscus sabdariffa* leaves in the green synthesis of ZnO NPs, as well as the characterization of the obtained material and its application in the photocatalytic degradation of methylene blue (MB).

2. Experimental details

2.1. Synthesis of ZnO nanoparticles

Hibiscus leaves were collected from College campus, (TBML College is located at: Porayar, Tranquebar (Tk), Nagapattinam (Dt), Tamilnadu, Porayar, Tamil Nadu, S. India Latitude: 11.0268187, Longitude: 79.8327422) washed and cut into pieces. It was boiled in distilled water for around an hour to get brown coloured leaf extract. The extract was filtered and preserved in the refrigerator. For the synthesis of zinc nanoparticles, 25 ml of leaf extracts was taken into a 250 ml beaker and boiled the extracts for 15 min at 60 – 80 °C using thermal control magnetic stirrer. 5 g of zinc nitrate was added to the solution when solution reached the temperature 60 °C. The mixture was then boiled until it reduced the Zn²⁺ ions and produced deep yellow coloured paste. Then the yellow paste was taken in a ceramic crucible and heated in furnace at four different temperatures 300, 400, 500 and 600 °C for 2 h. After cooling the crucible a light yellow coloured powder was obtained and this was carefully collected and stored in a zipper packet and used and saved for characterization. Whitish powder of ZnO nanoparticles formed in the crucible was removed from the furnace and crushed into a fine powder by using pestle and mortar.

2.2. Characterization

The materials were characterized and studied by different techniques. X-Ray Diffraction (XRD) was used to understand the crystal structure of the samples. Fourier-Transform Infrared Spectroscopy (FTIR) was used to study the functional groups present in the samples. Scanning Electron Microscopy (SEM) was used to study their morphology. Lastly, Ultra Violet-to-Visible spectroscopy (UV-Vis) for the study of the band gap of the samples, as well as the catalytic activity during the MB degradation.

2.3. Photocatalytic activity

The photocatalytic degradation activity of methylene blue (MB) dye solution was evaluated by the synthesized ZnO NPs. All the experiments were performed in the presence of sun light. Prior to the experiment, a suspension was arranged by adding 10 mg of synthesized ZnO NPs for different temperatures denoted as R₁ for 300 °C, R₂ for 400 °C, R₃ for 500 °C and R₄ for 600 °C. For each samples mixed with 100 ml of methylene blue (MB) dye solution in a 250 ml beaker placed on a magnetic stirrer at sunlight. Later, the mixture solution was kept in the dark for 10 min to set up the adsorption equilibrium. 5 ml reaction mixtures were taken at regular time interval (15 min) and centrifuged the solution for measurement. The absorption spectrum of the suspension mixture was measured periodically using an UV-visible spectrophotometer monitoring its absorption peak around 554 nm. The percentage of dye degradation was calculated using the following formula:

$$\frac{C_0 - C_t}{C_0} \cdot 100 \%,$$

where C_0 is the initial concentration of methylene blue, and C_t is the concentration of the dye at different time intervals.

3. Results and discussion

3.1. XRD analysis of ZnO nanoparticles

Figure 1 shows the XRD patterns of synthesized ZnO NPs. It reflects that all the diffraction peaks of ZnO NPs match with the standard Zn ONPs data. The X-ray diffraction patterns of the green synthesis NPs show different diffraction peaks at the 2θ values of 32.11, 34.76, 36.59, 47.85, 56.91 and 63.16 °; indexed to the (100), (002), (101), (102), (110) and (103) planes, respectively. These correspond to the hexagonal structure of the Wurtzite crystalline phase that is characteristic for ZnO NPs (JCPDS: 36-1451). For the diffraction pattern of the R₃ sample, rigid and narrow diffraction peaks are observed, indicating that it has a good crystalline structure. However, in the diffraction patterns of the samples R₁, R₂ and R₄ a decrease in the intensity and a widening of the diffraction peaks are observed, which is attributed to the decrease in the size of the crystals.

The crystal size can be calculated using the Debye–Scherrer formula [18]:

$$D = \frac{K\lambda}{\beta \cos \theta},$$

where D is the average size of the crystals, K is a dimensionless value (it is a constant approximately equal to 0.9), λ is the X-ray wavelength, β is the full width at half-maximum peak intensity (FWHM), and θ is the Bragg angle. The sizes of the crystals calculated from the XRD diffractograms were 38.33, 36.24, 28.01 and 32.12 nm for R₁, R₂, R₃ and R₄, respectively. These results indicate that the annealing temperature strongly influenced the crystallinity and the size of the crystals.

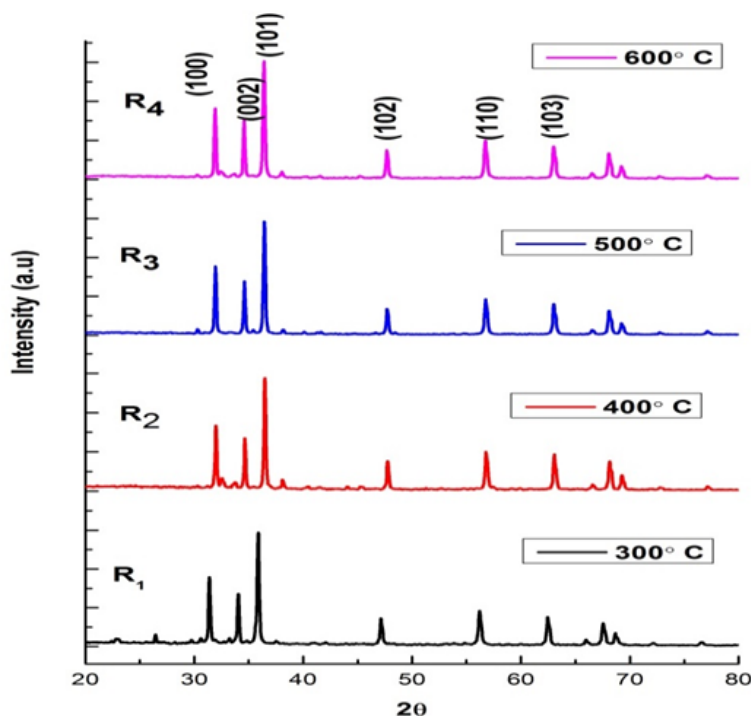


FIG. 1. XRD patterns of synthesized ZnO NPs

3.2. FTIR analysis

FTIR is an important tool to understand the functional groups and the relation between metal particles and biomolecules. The FTIR spectrums of *Hibiscus* leaf extract and synthesized ZnO NPs are shown in Fig. 2. The FTIR absorbance at 3408 cm^{-1} reveals the presence of O–H stretching vibration, a peak at 2927 cm^{-1} is due to C–H stretching vibration. It reveals that there are vibrational wavenumbers 865 , 1105 , 1495 , 2926 and 3445 cm^{-1} , corresponding to CH, C–OH, $\text{CH}_2\text{–OCH}_3/\text{CH}_2\text{–CH}_3$ and OH functional groups which are presented in the *hibiscus* extract in ZnO nanoparticles. The peak at 1614 cm^{-1} results from the stretching bands of C=O functional groups. Metal oxides generally give absorption in fingerprint region, i.e. below 1000 cm^{-1} arising from inter-atomic vibrations. The FTIR spectrum of the main absorption band is due to Zn–O stretching of ZnO in the range of $552\text{ – }417\text{ cm}^{-1}$. From the FTIR result the soluble elements presented in *hibiscus* extract could have acted as capping agent preventing the aggregate of nanoparticles in solution and laying a relevant role in their extracellular synthesis and shaping [19]. In addition to the absorption bands of the biomolecules used as reduction and stabilization (capping agents), the absorption peak at 440 cm^{-1} indicates the presence of ZnO NPs.

3.3. Morphological studies

The morphological structure and size of the ZnO NPs are analyzed by scanning electron microscopy (SEM). The SEM image of prepared ZnO NPs is shown in Fig. 3(a–d). The nanoparticles are mostly spherical in shape. SEM image of ZnO reveals that the sizes of the spherical nanoparticles are in the range of $20\text{ – }50\text{ nm}$.

The EDX spectrum of ZnO NPs shows peaks corresponding to Zinc and Oxygen. The atomic percentages of ZnO NPs are found to be 52.69 and 47.31% respectively as shown in Fig. 4.

3.4. Diffuse reflectance spectroscopy

Diffuse Reflectance Spectrum (DRS) of the synthesized ZnO nanoparticles were recorded at room temperature in the wavelength range of $190\text{ – }900\text{ nm}$. Kubelka–Munk (K–M (or) $F(R)$) formula [19] was used to determine the band gap of the materials. $F(R)$ was derived from the relation $F(R) = (1 - R)^2/2R$, where R is the reflection of the particles which is proportional to the extinction coefficient (α). Modified Kubelka–Munk formula can be derived by multiplying $F(R)$ by $h\nu$ where h is the Planck constant ($6.626 \cdot 10^{34}$ Joules) and ν is the light frequency (s^{-1}) associated with electronic transition. Plotting the value of $(F(R)h\nu)^2$ as a function of $h\nu$ one can find the direct band gap of ZnO nanoparticles. In the present work optical band gap of ZnO nanoparticles prepared from *Hibiscus* extract R₁, R₂, R₃ and R₄ is 3.24 , 3.21 , 3.28 and 3.22 eV respectively (Fig. 5(a, b)).

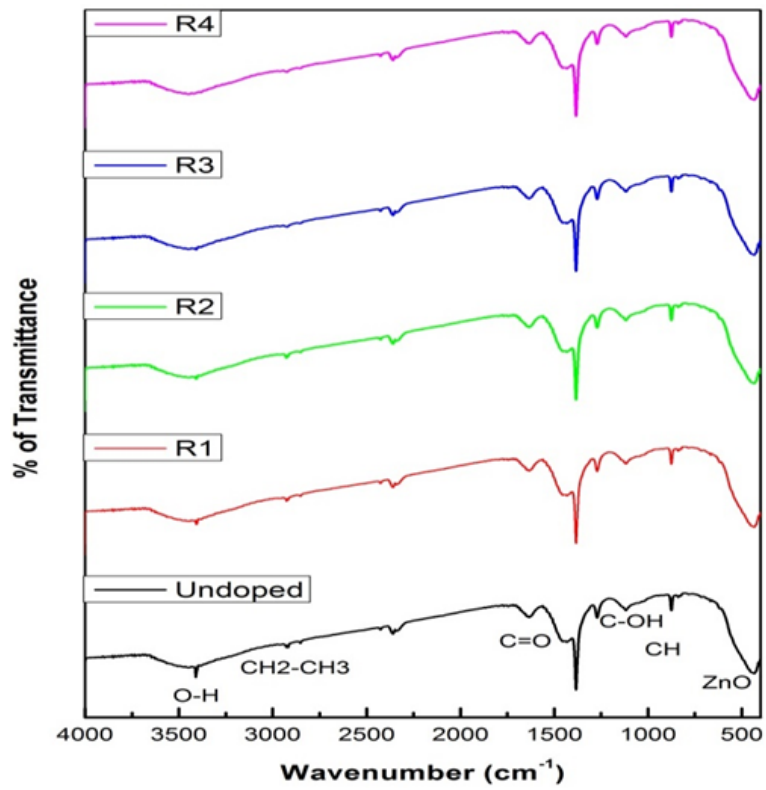


FIG. 2. FTIR spectrum of leaf extracted ZnO

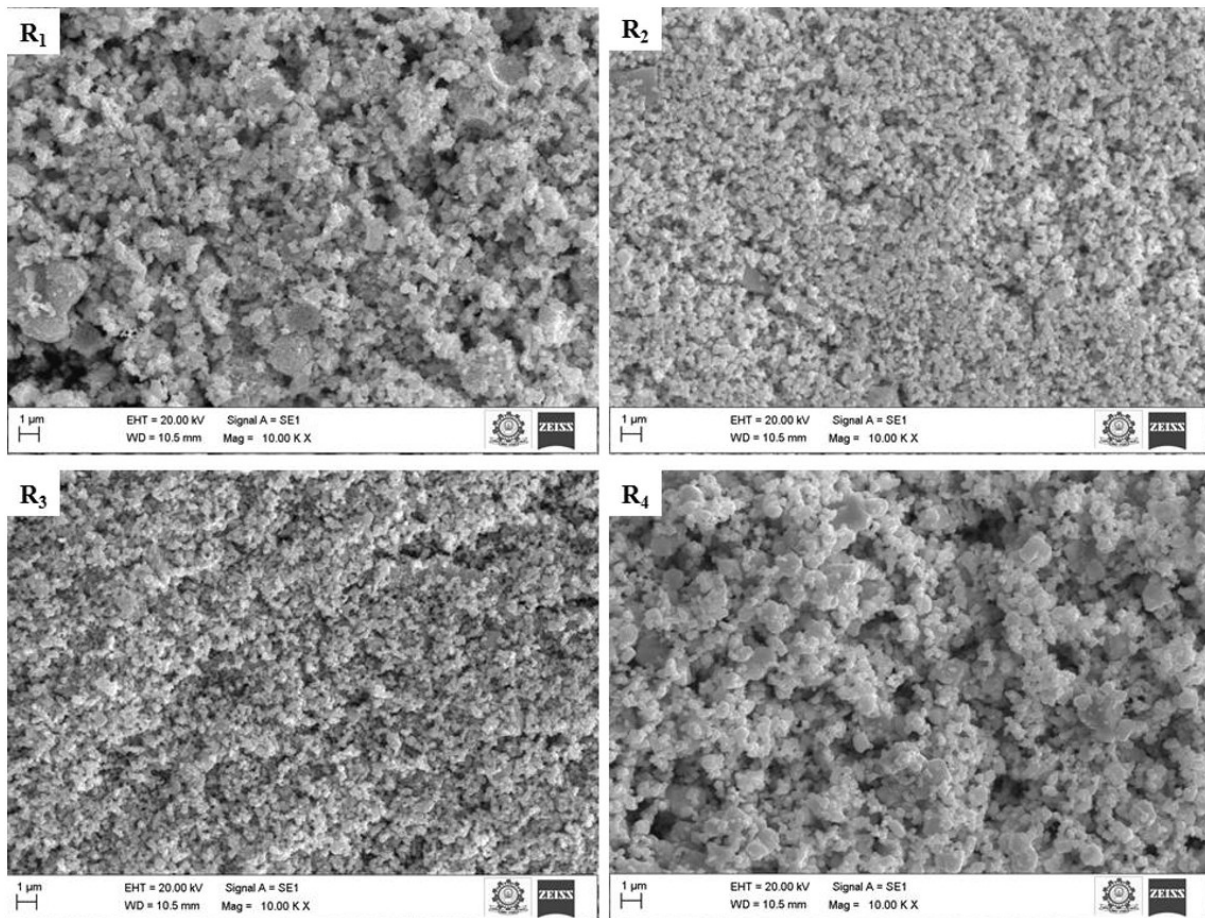


FIG. 3. The SEM image of prepared ZnO NPs

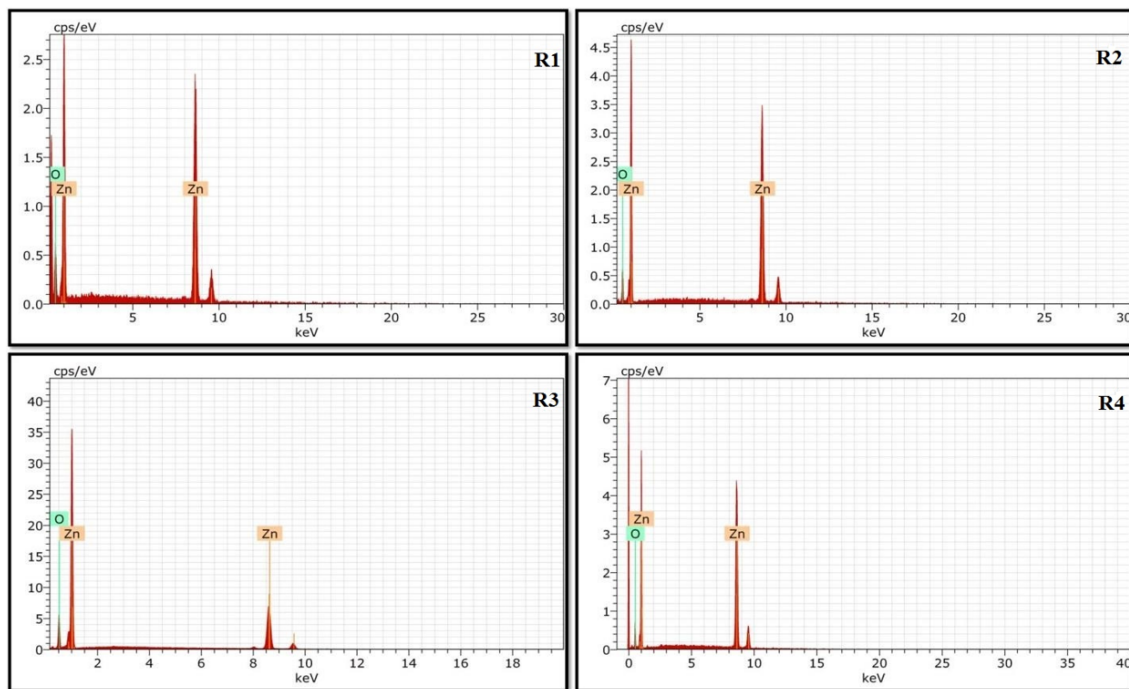
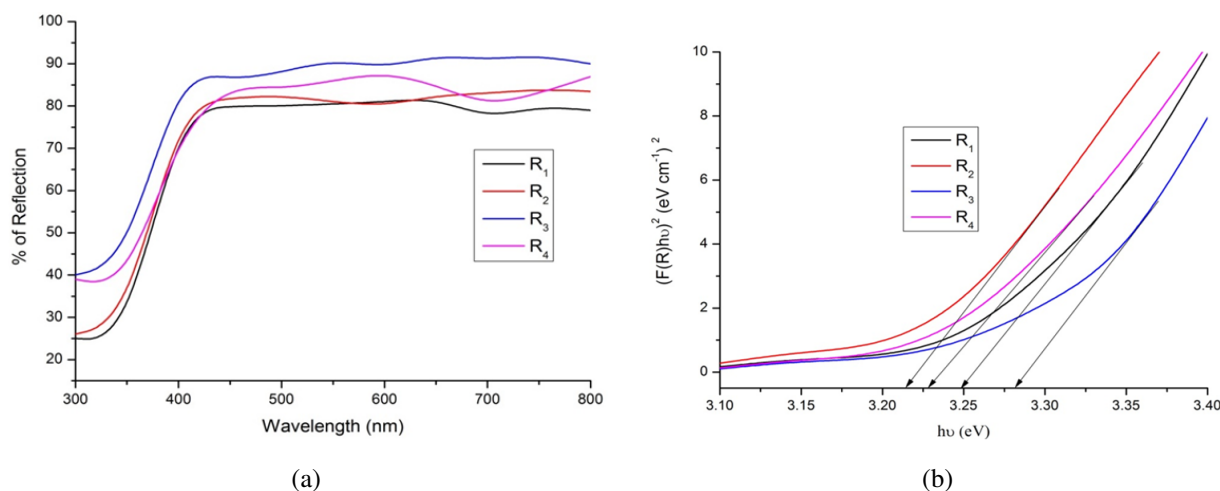


FIG. 4. The EDAX analysis of prepared ZnO NPs

FIG. 5. DRS of ZnO (a), TAUC plot of *hibiscus* leaf mediated ZnO NPs (b)

3.5. Photocatalytic activity

The photocatalytic dye degradation process 0.5 g of synthesized ZnO nanoparticles was added with 5 ppm of 100 ml of Methylene Blue (MB) solution. Initially MB dye absorption spectrum was recorded in the 190 – 1100 nm range using Shimadzu, UV-2600 spectrophotometer. Further, this solution was continuously stirred for 30 min to analyse adsorption and desorption equilibrium between catalyst and MB under dark condition. The stable aqueous dye solution was stirred and exposed under the sun light irradiation for 30 min. Then the experiment was carried out in the interval of 30 min and the UV-Vis absorption spectrum was recorded. Thus, the experiment was carried out for the total period of 120 min (one cycle) and the absorption spectrum was recorded at the interval of every 30 min. At the end of each cycle the dye solution was centrifuged to separate the ZnO nanoparticles and they were used without further treatment for next cycles.

ZnO nanoparticles synthesized from the Hibiscus extract solution of various annealed temperature (R_1 , R_2 , R_3 and R_4) were used in the degradation experiment of MB and the results of ZnO nanoparticles in the degradation of MB dye with respect to time (0 to 120 min) are shown in Fig. 6. The characteristic absorption peak of MB at 554 nm was chosen to monitor the photocatalytic degradation process. The degradation of MB dye is 57, 68, 94 and 73 % due to the ZnO nanoparticles prepared at R_1 , R_2 , R_3 and R_4 respectively as shown in Fig. 6(a-d). The degradation activity of ZnO

catalyst obtained from the precursor solution R₃ is relatively high when compared to the degradation activity of ZnO catalyst prepared from the other samples. It is shown in Fig. 7.

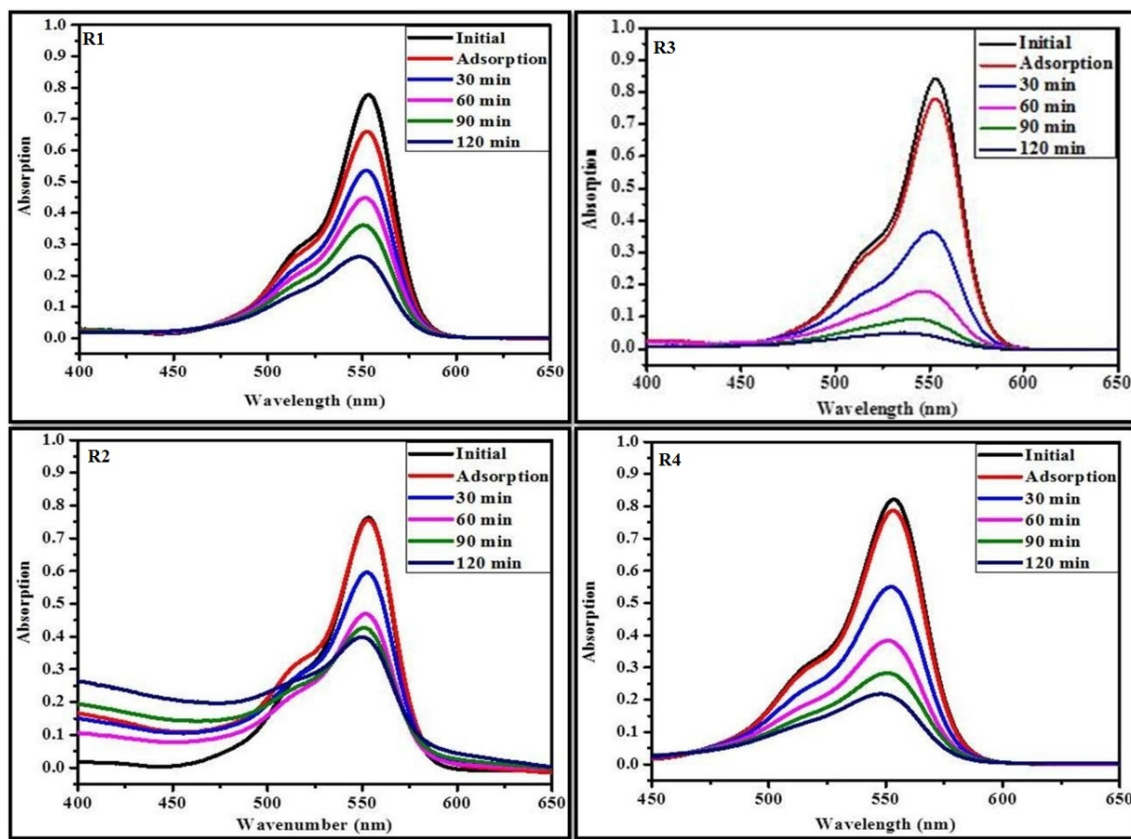


FIG. 6. Degradation effect of *hibiscus* leaf mediated ZnO NPs

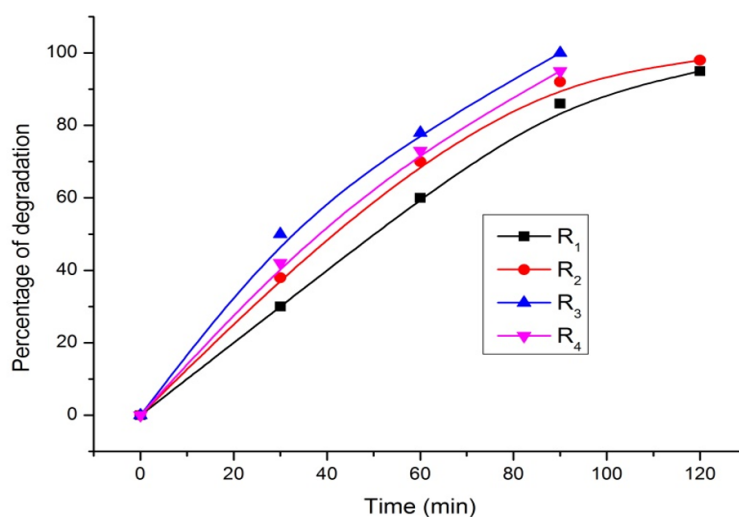


FIG. 7. Degradation Percentage of *hibiscus* leaf mediated ZnO NPs

The experiments prove that *hibiscus* leaf extract mediated ZnO improves the photocatalytic ability. In heterogeneous photocatalysis, when catalyst is irradiated with light with the photon energy greater than or equal to the band gap of catalyst, an electron from valence band jumps to the conduction band leaving a hole behind. Valence band hole reacts with water molecules to give $\cdot\text{OH}$ radicals and conduction band electron combines with adsorbed oxygen to give superoxide radical anion which further results in the formation of $\cdot\text{OH}$ radicals. The $\cdot\text{OH}$ radical is a strong oxidizing agent. It oxidizes dye molecules. This leads to its complete mineralization.

Temperature is one of the major factors that significantly influence the shape, size, stability, and yield of the NPs synthesized via a green route. Reaction temperature increase improves the reaction rate and high-temperature lead to increase of the nucleation rate. At high temperature, the NPs size was decreased. The underlying mechanism for green synthesis of ZnO NPs has not been fully understood as yet. Free amino and carboxylic groups of proteins, alkaloids, phenolics or avonoids, presented in the plant extract, may bind to the surface of zinc (Zn^{2+}) and trigger the formation of ZnO NPs. In heterogeneous photocatalysis, when catalyst is irradiated with light of photon energy greater than or equal to the band gap of catalyst, an electron from valence band jumps to the conduction band leaving a hole behind. Valence band hole reacts with water molecules to give OH radicals and conduction band electron combines with adsorbed oxygen to give superoxide radical anion which further results in the formation of OH radicals. The OH radical is a strong oxidizing agent. It oxidizes dye molecules. This leads to its complete mineralization

4. Conclusions

Synthesis of nanoparticles by using different parts of plants has been encouraged the designing of simple, green, cost and time effective approaches by minimizing the use of chemicals and solvents. Present study result highlights the effective use of leaf extract of Hibiscus rosasinesis towards synthesis of zinc oxide nanoparticles and their characterisation through XRD, SEM, UV-vis and FTIR study. The spherical structure and size (< 50 nm) of the synthesized nano ZnO is confirmed by SEM study. Moreover, XRD studies suggest that nano ZnO is absolutely crystalline in nature. The synthesized ZnO NPs (R_3) can be effectively used as an adsorbent which can remove approximately 94 % of methylene blue (MB) from aqueous solution. Therefore, it can be suggested that green synthesis of nano ZnO could be an alternative adsorbent for removal of dye from aqueous medium. Various efforts are being made to explore new materials as well as increasing the efficiency of existing bio adsorbents and designing of hybrid technologies targeting multicomponent bio adsorption. In future, bio adsorbents are poised to witness extensive applications at domestic and industrial scale to minimize the menace of environmental pollution. Moreover, the present study needs further field of application in order to explore more concrete information about the efficacy of this particular bio adsorbent.

References

- [1] Vacchi F.I., Vendemiatti J.A.d.S., et al. Quantifying the contribution of dyes to the mutagenicity of waters under the influence of textile activities. *Sci. Total Environ.*, 2017, **601–602**, P. 230–236.
- [2] Ghaffar A., Zhang L., Zhu X., Chen B. Porous PVdF/GO Nanofibrous Membranes for Selective Separation and Recycling of Charged Organic Dyes from Water. *Environ. Sci. Technol.*, 2018, **52**, P. 24265–4274.
- [3] Gaya U.I., Abdullah A.H. Heterogeneous photocatalytic degradation of organic contaminants over titanium dioxide: A review of fundamentals, progress and problems. *J. Photochem. Photobiol. C*, 2008, **9**, P. 21–12.
- [4] Janoš P. Sorption of Basic Dyes onto Iron Humate. *Environ. Sci. Technol.*, 2003, **37**, P. 5792–5798.
- [5] Pal B., Kaur R., Grover I.S. Superior adsorption and photodegradation of eriochrome black-T dye by Fe^{3+} and Pt^{4+} impregnated TiO_2 nanostructures of different shapes. *J. Ind. Eng. Chem. (Amsterdam, Neth.)*, 2016, **33**, P. 2178–184.
- [6] Santhosh C., Velmurugan V., et al. Role of nanomaterials in water treatment applications: A review. *Chem. Eng. J.*, 2016, **306**, P. 21116–1137.
- [7] Shaari N., Tan S., Mohamed A. Synthesis and characterization of CNT/Ce-TiO₂ nanocomposite for phenol degradation. *J. Rare Earths*, 2012, **30**, P. 2651–658.
- [8] Pardeshi S.K., Patil A.B. Effect of morphology and crystallite size on solar photocatalytic activity of zinc oxide synthesized by solution free mechanochemical method. *J. Mol. Catal. A: Chem.*, 2009, **308**, P. 232–240.
- [9] Ahmad M., Ahmed E., et al. Enhanced photocatalytic activity of Ce-doped ZnO nanopowders synthesized by combustion method. *J. Rare Earths*, 2015, **33**, P. 2255–2262.
- [10] Cerrato E., Gionco C., Paganini M.C., Giamello E. Photoactivity properties of ZnO doped with cerium ions: an EPR study. *J. Phys.: Condens. Matter*, 2017, **29**, 444001.
- [11] Samadi M., Zirak M., et al. Recent progress on doped ZnO nanostructures for visible-light photocatalysis. *Thin Solid Films*, 2016, **605**, P. 2–19.
- [12] Maryanti E., Damayanti D., Gustian I., Yudha S.S. Synthesis of ZnO nanoparticles by hydrothermal method in aqueous rinds extracts of Sapindus rarak DC. *Mater. Lett.*, 2014, **118**, P. 296–298.
- [13] Zak A.K., Abrishami M.E., et al. Effects of annealing temperature on some structural and optical properties of ZnO nanoparticles prepared by a modified sol-gel combustion method. *Ceram. Int.*, 2011, **37**, P. 2393–2398.
- [14] Jamal R.K., Hameed M.A., Adem K.A. Optical properties of nanostructured ZnO prepared by a pulsed laser deposition technique. *Mater. Lett.*, 2014, **132**, P. 231–233.
- [15] Zak A.K., Majid W.H.A., et al. Sonochemical synthesis of hierarchical ZnO nanostructures. *Ultrason. Sonochem.*, 2013, **20**, P. 2395–2400.
- [16] Ao W., Li J., et al. Mechanochemical synthesis of zinc oxide nanocrystalline. *Powder Technol.*, 2006, **168**, P. 2148–2151.
- [17] Salavati-Niasari M., Davar F., Khansari A. Nanosphericals and nanobundles of ZnO: Synthesis and characterization. *J. Alloys Compd.*, 2011, **509**, P. 261–265.
- [18] Porkalai V., Sathya B., Benny Anburaj D., Nedunchezian G. Effect of calcinations on the structural and morphological properties of Ag and In co doped ZnO nanoparticles. *J. Mater. Sci.: Mater. Electron.*, 2017, **28**, P. 22521–22528.
- [19] Stone F.S. UV-Visible Diffuse Reflectance Spectroscopy Applied to Bulk and Surface Properties of Oxides and Related Solids. In Bonnelle, J.P., Delmon, B., Derouane, E. (eds) *Surface Properties and Catalysis by Non-Metals*, NATO ASI Series, Springer, Dordrecht, 1983, **105**, P. 2237–2272.

Information about the authors:

S. Roselin Mariyal – P.G. and Research Department of Physics, D.G. Govt Arts College (Affiliated to Bharathidasan University), Mayiladuthurai, India

G. Nedunchezhian – P.G. and Research Department of Physics Thiru. Vi. Ka. Govt Arts College (Affiliated to Bharathidasan University), Thiruvarur, India

D. Benny Anburaj – P.G. and Research Department of Physics, D.G. Govt Arts College (Affiliated to Bharathidasan University), Mayiladuthurai, India

S. Joshua Gnanamuthu – P.G. and Research Department of Physics, TBML College (Affiliated to Bharathidasan University), Porayar, India; joshuagnanamuthu@gmail.com

Conflict of interest: the authors declare no conflict of interest.